Reprinted from *American Laboratory* April 2010

Technical Article

by Terry C. Chilcott, Hans G.L. Coster, and Jeffrey L. Ellis

Structural, Compositional, and

Topographical Characterization of Polystyrene Films Using High-Resolution Dielectric Spectroscopy

Thin polymeric films and surfaces provide novel electrochemical, thermal, mechanical, and/or biocompatible features at the nanoscale level in the development of adhesives, protective coatings, lubricants, and suspension stabilizers, as well as in semiconductor devices such as biosensors used in medicine.

The interface between the film and substrate principally determines the structural and thermodynamic stability of multiphase polymer systems, and the interface between the film and external environment determines the specialized functionality of the film. A comprehensive understanding of the thermodynamics at the nanoscale level is crucial to the development of better manufacturing practices that strengthen film–substrate interfaces and accentuate the functionality of film–environment interfaces.

High-resolution electrical impedance spectral studies on silicon

Silicon wafers provide surfaces that are suitably flat at the atomic level for dielectric spectral (DS) characterizations of the structural and topographical features of nanostructures. *Figure 1* illustrates the dielectric spectrometer and details the characterization chamber (**Inphaze Pty. Ltd.**, Sydney, Australia), into which functionalized surfaces are mounted. The system's design[3] ensures a uniform density of the alternating current stimulus, *i*, that enables full utilization of the 24-bit acquisition of the response, *v*, and yields better than one-thousandth of a degree resolution in phase at frequencies as low as one-thousandth of a Hertz.[4] Angstrom resolutions have been achieved with the **Inphaze** technology on silicon[2] and gold.[1]

Theoretical background

Dielectric characterization is broadly based on the degree to which the electrical properties of a nanostructure of dielectric constant, ε_r, and thickness, *d*, depart from those

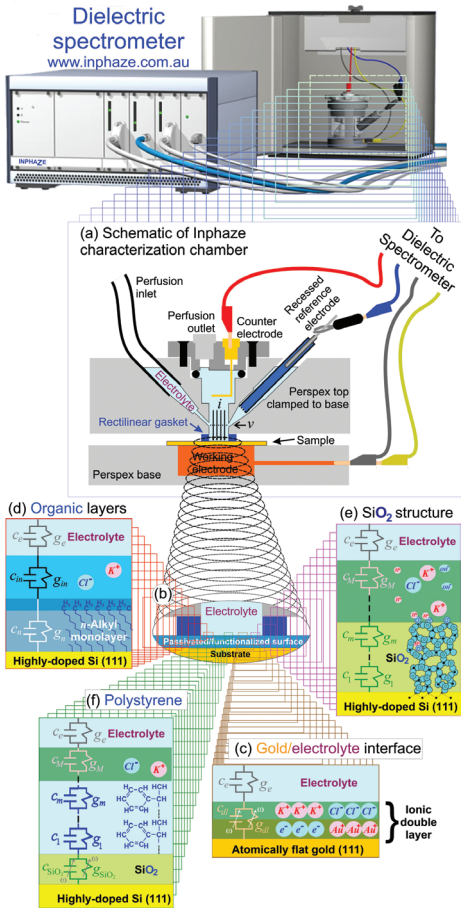

Figure 1 ***Inphaze*** *dielectric spectrometer and characterization chamber illustrating a) the three-terminal configuration for characterizing b) functionalized nanostructures on substrates such as c) gold,[1] d) silicon,[2] and e and f) silicon dioxide. c, d, e, and f) A spectrum of measurements is modeled by a series of electrical circuit elements, each comprising a conductive (g) and capacitive (c) component. a) Gallium-indium eutectic was applied to the underside of silicon samples to form a low-ohmic contact with the working electrode with functionalized surfaces facing upward. A gearing mechanism regulated by springs (not shown) was used to lower a gasket of rectilinear cross-section onto functionalized surfaces and delicately seal a precisely defined "active" area while minimizing distortion of the surface at the gasket perimeter. Electrolyte was perfused into the inner space of the chamber, wetting the active surface as well as the counter and reference electrodes. The working and counter electrodes injected a sinusoidal current of amplitude, i, and angular frequency, ω, through the surface. The recessed reference electrode monitored the voltage response of amplitude, v, and phase, ø (referenced to that of i). The capacitance and conductance of the system are given by* $i\sin(-\phi)/\omega/v$ *and* $i\cos(-\phi)/v$*, respectively.*

of an ideal parallel plate capacitor, the capacitance (per area) of which is given by:

$$c \equiv \frac{\varepsilon_r \varepsilon_o}{d} \qquad (1)$$

where ε_o is the dielectric permittivity of free space (= 8.85 10^{-2} Fm^{-1}). Real capacitors leak electric charge with a characteristic time constant given by:

$$\tau \equiv \frac{c}{g} \qquad (2)$$

where *g* denotes the leak conductance, which is 0 for an ideal capacitor. The reciprocal time constant yields a characteristic frequency given by:

$$\omega_{constant} \equiv \frac{g}{c}$$

or

$$f_{constant} \equiv \frac{\omega_{constant}}{2\pi} = \frac{g}{2\pi c} \qquad (3)$$

below which the electrical properties are dominated by the leak conductance.

Dielectric characterization of a monolayer and bilayer

Figure 2a shows the measured capacitance of an octadecane monolayer on a highly conducting atomically flat silicon substrate in contact with a 100 mM KCl electrolyte. The fitted curve was generated using the shown values for the parallel plate capacitor, c_2, the leak conductance, g_2, and the series conductance, g_1, representing the electrolyte. The value for c_2 is given by those measurements below 200 Hz that are characterized by the frequency independence

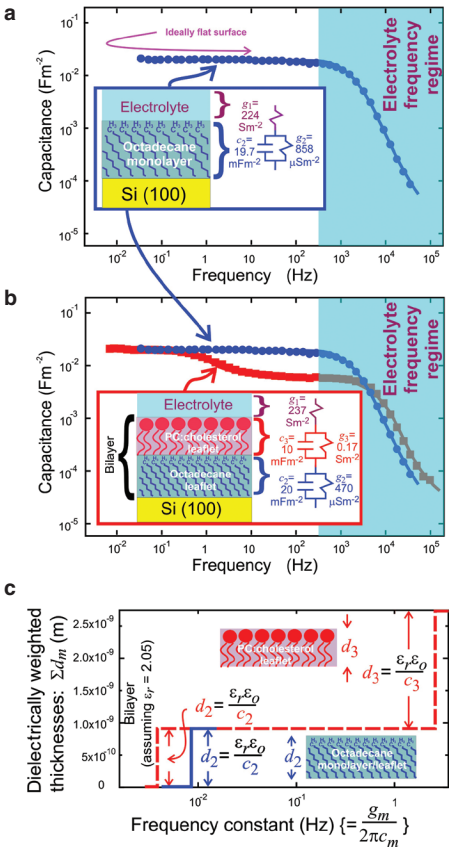

Figure 2 *Dielectric characterizations of a monolayer and bilayer (adapted from Ref. 2). a) The capacitance dispersion with frequency (•) of an octadecane monolayer on highly doped silicon in contact with a 100 mM KCl solution. Hydrosilylation chemistry in octadecene under UV light in a deoxygenated environment linked the octadecane monolayer via Si–C bonds to a hydride-terminated surface of a p-type Si(100) wafer of resistivity 0.005 Ωcm after the removal of silicon dioxide using hydrofluoric acid. b) Comparison of the capacitance dispersion in (a) with that obtained after the formation of a phosphatidylcholine:cholesterol leaflet on the octadecane surface (■) using the vesicle adsorption technique. c) Structural line-spectra for the monolayer (——) and bilayer (---), which feature a step for each monolayer characterized by the* ***Inphaze*** *analysis of the spectra in (a) and (b) (see Refs. 5 and 6). The height of the step corresponds to the thickness of the monolayer (assuming ε_r = 2.05), and its location corresponds to the frequency constant. An additional step corresponding to electrolyte is not shown.*

predicted by Eq. (1). Equations (1) and (3) yield estimates of the thickness d_2 (assuming ε_r = 2.05) and the frequency constant that were consistent with those expected for the monolayer,[2] and are represented in the structural line-spectrum shown in Figure 2*c* as a step in thickness at this frequency constant value.

Figure 2*b* reveals the manifestation of a second constant capacitive regime in the frequency range of 10–10^3 Hz after vesicles of phosphatidylcholine:cholesterol (2:1 mol/mol) were placed onto the monolayer. This manifestation is accommodated in the model for the monolayer alone by the series addition of an ideal capacitor, c_3, and its leak conductance, g_3, which is consistent with the vesicles adsorbing to the octadecane surface to form a second monolayer. Figure 2*c* shows that the structural line-spectrum for the bilayer (---) contains two steps. The step characterized by the lowest frequency constant is very similar in height and location to the step obtained for the octadecane monolayer alone (——), indicating that it characterizes the thickness (assuming ε_r = 2.05) and frequency constant for the base leaflet of the bilayer comprising octadecane. Thus, the second step characterized by a frequency constant value that is two orders of magnitude greater than that of the monolayer characterizes the phosphatidylcholine:cholesterol upper leaflet.

Dielectric characterization of native silicon oxide surfaces

Figure 3a shows that capacitance measurements for a silicon dioxide "layer" (◊) disperse continuously with frequency over the frequency range at which distinctive plateaus in capacitance dispersions shown in Figure 2 previously identified the presence of two electrically specific layers. The continuous dispersion is that expected for several electrically distinct sublayers. This is consistent with extensive studies reviewed by Grunthaner and Grunthaner[7] involving a variety of techniques including X-ray photoelectron spectroscopy (XPS), nuclear magnetic resonance (NMR), contact angle measurements, ellipsometry, and surface extended X-ray absorption fine structure (SEXAFS). These studies show that the silicon dioxide layer indeed comprises five to six sublayers in which SiO_4 tetrahedrons bridged by the oxygen atoms form regular ringed cages comprising four tetrahedrons approx. 4.3 Å in size next to the Si(111)/SiO_2 interface, transitioning to eight tetrahedrons approx. 7.8 Å in size at the SiO_2 surface. The dielectric characterization identified these sublayers, as illustrated in the structural line-spectrum (——) shown in *Figure 4*, in which the steps have been reordered such that thickness values of layers (assuming ε_r = 4.4) increase toward the surface in concert with cage size.

The dielectric characterization further reveals that the frequency constant values taper away from the value attributed to the Si(111)/SiO_2 interface, consistent with the density of sites where silicon interacts with dopant to promote electrical conduction, decreasing with increasing cage size. The sharp increase in the value for the sublayer at the surface is consistent with the permeation of highly conducting electrolyte into the voids of the SiO_2 cages increasing with increasing cage size.

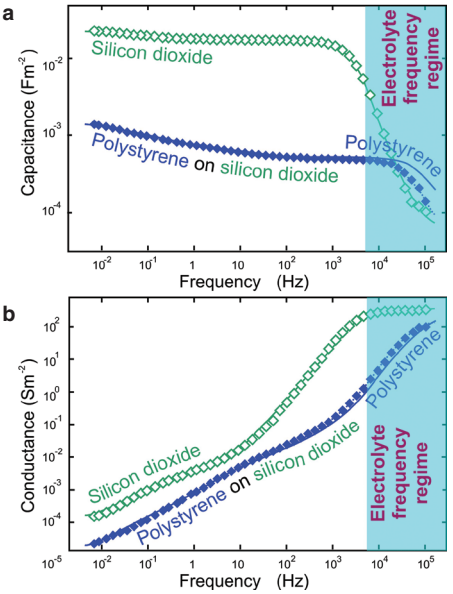

Figure 3 *Measured capacitance (a) and conductance (b) dispersions with frequency of a native silicon dioxide layer on highly doped silicon (◊) and polystyrene on that silicon dioxide layer (♦) while in contact with a 100 mM KCl electrolyte. The theoretical plot for the polystyrene layer alone (——) differs marginally from that fitted to measurements of the polystyrene layer on the silicon dioxide layer (---). Highly doped silicon wafers were cleaned in piranha solution for 25 min at 90 °C, rinsed with Milli-Q ultrapure water (****Millipore Australia Pty. Ltd.****, North Ryde, Australia), and air-dried. Polystyrene was dissolved in toluene at concentrations between 0.25 and 1.0 wt % and spun-coated onto the silicon wafers using a G3P-8 Spincoater (****Specialty Coating Systems,*** *Indianapolis, IN) at 2500 rpm for 70 sec. The toluene was allowed to evaporate in ambient conditions for at least 24 hr, after which the sample was annealed at 130 °C in a vacuum for at least 12 hr.*

Dielectric characterization of polystyrene on silicon dioxide

Figure 3 further shows an order of magnitude decrease in the measured capacitance and conductance after a polystyrene film was spun-coated onto the SiO_2 surface. It additionally illustrates an increase in the extensiveness of the capacitance dispersion expected from the addition of further layers. These differences are more precisely reflected in Figure 4, which reveals a structural line-spectrum for polystyrene (---) that features more steps than that

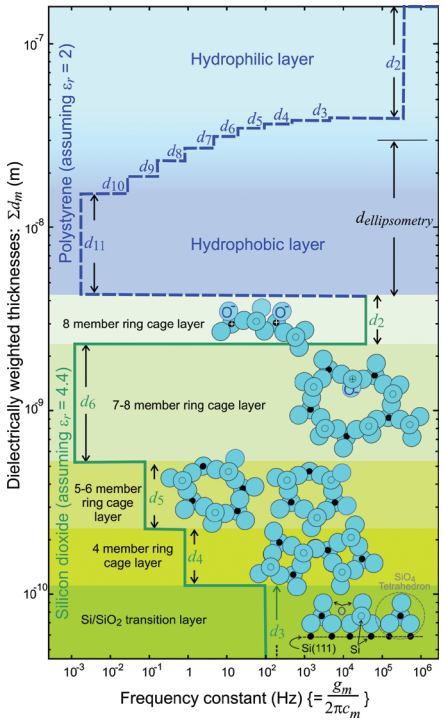

*Figure 4 Structural line-spectrum for silicon dioxide (——) correlated with caged networks of SiO_4 tetrahedrons, which increase in number from four at the Si(111)/SiO_2 interface to eight at the surface (see Ref. 7). The spectrum for polystyrene (– – –) reveals a substantial hydrophobic layer at the SiO_2/polystyrene interface, terminating in a substantial hydrophilic layer at the surface. An additional step corresponding to electrolyte is not shown. Also, $d_{ellipsometry}$ is the measurement of the bulk thickness of the polystyrene film using an M-2000V spectroscopic ellipsometer (**J.A. Woollam Co., Inc.**, Lincoln, NE).*

for silicon dioxide (——), which in turn features more steps than those spectra shown in Figure 2*c* for the bilayer (– – –), which features two steps, and the monolayer (——), which features only one step.

The structural line-spectra thus provide a basis for distinguishing between the compositional and structural features of these nanostructures. But the detail also reveals compositional and structural similarities, such as the similar contributions of octadecane to the spectra as a monolayer and as a leaflet in a bilayer. Further, the conductivity (= *gd*) and frequency constant values for octadecane are similar to those values for the sublayer of thickness denoted by d_{11} for polystyrene in Figure 4, which is consistent with octadecane and this polystyrene sublayer sharing an unsaturated hydrocarbon backbone, as illustrated in Figure 1*d* and *f*. Furthermore, the conductivity values are characteristic of the known insulating properties of hydrocarbon structures and hydrophobic interactions of these structures with an electrolyte that exclude water molecules, including those molecules that hydrate the ions.

The frequency constant value for the polystyrene sublayer of thickness denoted by d_2 is at least an order of magnitude larger than values for any of the other polystyrene sublayers and more characteristic of the hydrophilic properties of the electrolyte than the hydrophobic properties of polystyrene. Further, the value for d_2 even when assuming ε_r = 2 is much larger than the measurement of 290 Å for the bulk thickness of the film using ellipsometry, consistent with this sublayer reflecting properties of a region external to the film, i.e., the film–electrolyte interface.

The frequency constant values for the remaining polystyrene sublayers span the value characterizing the hydrophobic properties of the film and the value characterizing the hydrophilic properties of the interface. This is consistent with these sublayers also reflecting the absorbance of highly conducting electrolyte that would be expected to increase as the density of polystyrene tapers toward the film surface.[8–10] Indeed, the sum of the thickness values for $d_{10},\ldots,d_3$ (assuming ε_r = 2) is of comparable magnitude to estimates from the literature of the extent to which this transition in density occurs (i.e., 80–130 Å; see Refs. 11 and 12), and is consistent with reported topographical studies of metal surfaces that correlate the degree of roughness as characterized by atomic force microscopy (AFM) with the extensiveness and steepness of capacitance dispersions with frequency.[1]

Most importantly, the sum of the thickness values for $d_{11},\ldots,d_3$ yields a total thickness for the polystyrene film that is shown in Figure 4 to be of comparable magnitude to the estimate provided by ellipsometry.

Conclusion

The high-resolution **Inphaze** impedance characterization identified a hydrophobic sublayer in the polystyrene film and a series of sublayers with electrochemical and geometrical properties consistent with that expected for a transition region in which the density of polystyrene tapered toward the film surface. The sum of the thicknesses for these sublayers was comparable with the measurement of the bulk thickness of the same film using ellipsometry. Significantly, the dielectric characterization encompassed compositional, structural, and topographical detail provided by a variety of highly sophisticated techniques commonly used to characterize nanostructures and surfaces of multiphase polymer systems.[13] Further, characterization of the interface with an external aqueous environment was facilitated, illustrating that dielectric characterizations can additionally monitor in situ interactions of surfaces with environments that multiphase polymer systems are designed to enhance.

References

1. Chilcott, T.C.; Wong, E.L.S.; Coster, H.G.L.; Coster, A.F.C.; James, M. *Electrochim. Acta* **2009**, *54*, 3766–74.
2. Chilcott, T.C.; Wong, E.L.S.; Böcking, T.; Coster, H.G.L. *Physiol. Meas.* **2008**, *29*, S307–19.
3. Coster, H.G.L.; Chilcott, T.C. Apparatus for electrochemical characterizations. PCT application filed in Germany (2006), and internationally (2007).
4. Coster, H.G.L.; Chilcott, T.C. An improved method of measuring the phase difference between arbitrary periodic waveforms. PCT application filed in Australia, 2006.
5. Coster, H.G.L.; Chilcott, T.C.; Coster, A.C.F. *Bioelectrochem. Bioenergetics* **1996**, *40*, 79–98.
6. Karolis, C.; Coster, H.G.L.; Chilcott, T.C.; Barrow, K.H. *Biochim. Biophys. Acta* **1998**, *1368*, 247–55.
7. Grunthaner, F.J.; Grunthaner, P.J. *Mat. Sci. Rep.* **1986**, *1*(2), 65–160.
8. Mansfield, K.F.; Theodorou, D.N. *Polym. Prepr.* **1989**, *30*(2), 76–7.
9. Mansfield, K.F.; Theodorou, D.N. *Macromolecules* **1991**, *24*(23), 6283.
10. Mayes, A.M. *Macromolecules* **1994**, *27*(11), 3114.
11. Keddie, J.L.; Jones, R.A.L.; Cory, R.A. *Europhys. Lett.* **1994**, *27*(1), 59.
12. Forrest, J.A.; Dalnoki-Veress, K.; Dutcher, J.R. *Phys. Rev. E: Stat. Phys.* **1997**, 56(5-B), 5705.
13. Yang, Y.; Cheng, M.M.-C.; Hu, X.; Liu, D.; Goyette, R.J.; Lee, L.J.; Ferrari, M. *Macromolecules* **2007**, *40*(4), 1108.

Dr. Chilcott and Prof. Coster are with the School of Chemical and Biomolecular Engineering, University of Sydney, NSW 2006, Australia; tel.: +61 408463761; fax: +61 293512854; e-mail: terry.chilcott@sydney.edu.au.

Mr. Ellis was supported at the University of Sydney by a National Science Foundation (EEC-0425626) grant to Prof. David L. Tomasko, Department of Chemical and Biomolecular Engineering, Ohio State University, Columbus, OH, U.S.A., and an International Research and Education in Engineering Travel Grant (0738464).